

RESERVOIR CHARACTERIZATION OF THE UPPER CRETACEOUS ABU ROASH 'G' MEMBER, USING WIRELINE LOG AND 3-D SEISMIC DATA IN HAMRA OIL FIELD, WESTERN DESERT, EGYPT

M. Abulhassan⁽¹⁾, M. Farouk⁽¹⁾ and G. Elsayed⁽²⁾

(1) Geology Department, Faculty of Science, Menofiya University, Egypt.

(2) Exploration Department, Qarun Petroleum Company, Egypt.

توصيف خزان الطباشيري العلوي لطبقة أبو رواش 'G' ، باستخدام تسجيلات الآبار والبيانات السيزمية
ثلاثية الأبعاد في حقل حمرا، الصحراء الغربية، مصر

الخلاصة: تهدف هذه الدراسة إلى الربط والتحليل بين تسجيلات الآبار والبيانات السيزمية ثلاثية الأبعاد لأربعة آبار لتقييم طبقة رمال أبو رواش (G) الوسطي والسفلي في حقل حمرا النفطي ، الصحراء الغربية ، مصر .
تم إجراء التفسير على الخطوط السيزمية وتحليل البيانات البتروفيزيائية للتسجيلات الكهربية لأربع آبار مستخرجة من حقل الحمرا حيث تم تحديد وتقييم رمال أبو رواش (G) الوسطي والسفلي من خلال إنشاء خرائط مختلفة مثل الخرائط التركيبية ، الرملية ، المتوسط الحسابي لتشبع المياه وخرائط المسامية. تم التعرف على عدد من الصدوع الطبيعية والتي كان الاتجاه السائد لها هو شرق-غرب وشمال شرق-جنوب غرب والتي أدت إلى تكوين بعض المناطق العالية التي مثلت المصائد البتروولية ثلاثية الاتجاهات في منطقة الدراسة.
أظهرت نتائج الدراسة أن رمال أبو رواش (G) الوسطي لديها خصائص مكملة أفضل من رمال أبو رواش (G) السفلي حيث أنه تتراوح خواصه البتروفيزيائية في منطقة الدراسة بين حوالي 22% و 33% للمسامية الفعالة ، وتتراوح بين حوالي 6% و 12% للمحتوى الطيني و حوالي 34% و 48% لدرجة التشبع بالمياه بينما تتراوح في رمال أبو رواش (G) السفلي بين 16% و 34% من أجل المسامية الفعالة ، تتراوح بين 4% و 26% للمحتوى الطيني ، وتتراوح بين حوالي 52% و 100% لدرجة التشبع بالمياه. كل هذه النتائج تشير إلى أن تكوين أبو رواش في هذا الحقل يمكن اعتباره مكملاً جيداً إذا إمكانية عالية لإنتاج النفط. بناءً على هذه النتائج تم حساب حجم الزيت الأصلي المتواجد في كل من الخزانات المذكورة بإجمالي قدر بحوالي 28 مليون برميل زيت.

ABSTRACT: The present work focuses on well logs interpretation for evaluating the Middle Abu Roash G sand Member, and the Lower Abu Roash G sand Member in Abu Roash Formation in Hamra oil field. This study has been carried out by the integration and interpretation of the well-logging analysis and the 3-D seismic data of four wells distributed in the Hamra oil field.

The study results show that the Middle Abu Roash G sand Member has better reservoir characterization than the Lower Abu Roash sand Member. The estimated petrophysical parameters of the reservoir throughout the study area for the Middle Abu Roash G sand Member range between about 22% and 33 % for the effective porosity, and range between about 6 % and 12 % for shale volume, and range between about 34 % and 48 % for Water saturation, and while range in the Lower Abu Roash sand Member between about 16 % and 34 % for effective porosity and between about 4 % and 26% for shale volume, range between about 52 % and 100 % for Water saturation. All of these results indicate that Abu Roash G Formation in this field can be considered as good reservoir with high potential for oil production.

1. INTRODUCTION

Hydrocarbon occurrence in the Western Desert is closely related to the tectonic activities and stratigraphic history of the area which has created a series of reservoirs and seals. Most fields in the northern Western Desert are related to structures formed in Late Cretaceous-Eocene and are placed in or at the edge of early depo-centers that later became kitchen areas (Abu El Naga, 1984). Most of the sedimentary basins in Egypt are located in the northern Western Desert e.g. Matruh- Shushan basin, North Meleha basin, Alamein basin, Abu Gharadig basin (of our interest), Gindi basin, Beni Suef basin, and Paleozoic Basins Workflow. Abu Gharadig basin includes a huge number of oil, gas, and oil and gas fields in its depo-center and troughs; such as Abu Gharadig field, North Abu Gharadig field, Badr El-

Din (BED) lease, GPT field, Wadi field (WD 33), Asala platform, Diyur field, and Karama lease, Raham lease in which Hamra oil field exist.

2-Aim of the present study

This study aims to integrate between well log interpretation analysis for evaluating the Middle and Lower Abu Roash G sand Member in Abu Roash Formation in Hamra oil field, Western Desert, Egypt. Which reservoir characterization is one of the most important steps in exploration and development phase of any prospect. It combines the results of the different analyses to optimize production, reduce risk, uncertainties and enhance understanding of the reservoir. So the aim of the study to calculate the qualitative and quantitative well-logging data

interpretation. Formation evaluation is enhanced by gathering the available electrical logs for the studied wells and calibrating them for different environmental effects, then carrying out the different calculation processes for different reservoir parameters, and finally the presentation of the resulting data through crossplots, and aerial distribution maps.

3- Materials and Methodology

Interpretation was conducted for seismic lines and (GR, Resistivity, Density and Neutron) logs of four wells extracted from Hamra field (Fig. 1). Integrated methods involving seismic interpretation and petrophysical data analysis were employed to meet the objectives of this study. Interpretations of seismic sections were done, the Middle and Lower Abu Roash G sand Member were identified and evaluated by generating various maps such as structural, net reservoir thickness, arithmetic average water saturation and arithmetic average effective porosity maps.

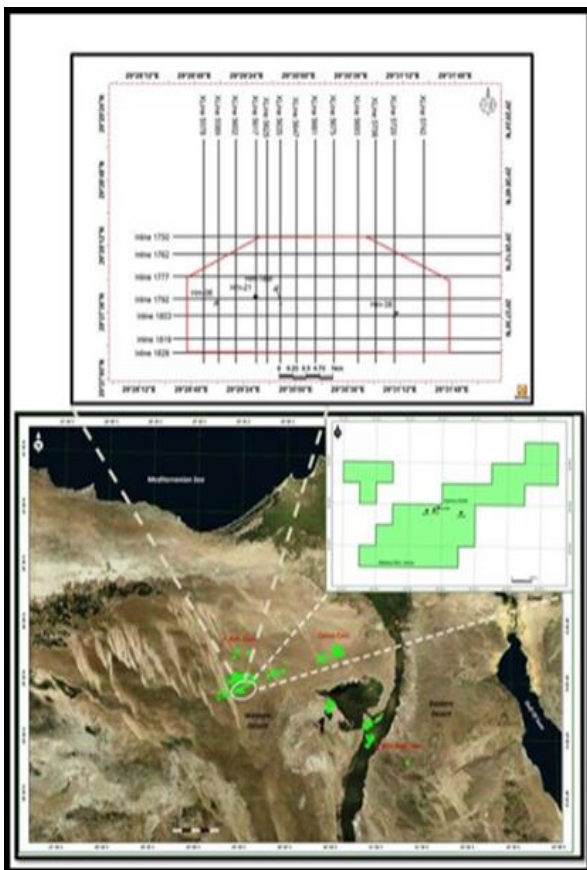


Fig. (1): location map of Hamra field North Western Desert.

4-Geological Setting

Stratigraphic setting

The stratigraphic section of the North Western Desert is thick and includes most of the sedimentary succession from recent to Pre-Cambrian basement complex (Schlumberger, 1995). (Fig.2).

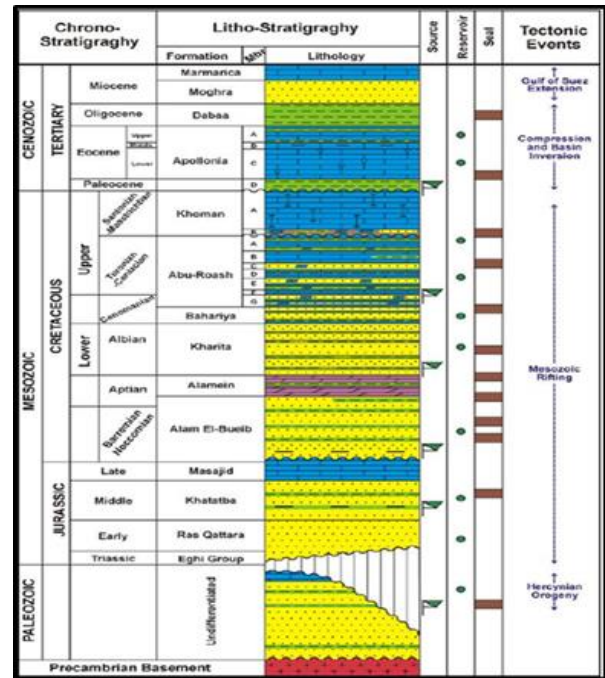


Fig. (2): Generalized stratigraphic column of the north Western Desert of Egypt. (After, Moustafa, et al., 2003).

The sedimentary sequence of the study area based on deepest drilled well ranges in age from the Early Jurassic Ras Qattara Formation to Miocene Moghra Formation at surface. The Cretaceous mega-sequence is divided into Lower and Upper sequences, the Lower Cretaceous includes Alam El Bueib, Alamein, Dahab and Kharita formations while the Upper Cretaceous sequence incorporates Bahariya, Abu Roash and Khoman formations (Hantar, 1990).

The Late Cretaceous Abu Roash “G” Member represent the main reservoirs in the study area, it is a Late Cenomanian in age (Abdel Aal, 1990). It is heterogeneous both vertically and laterally, and becomes sandy through Abu Gharadig basin (Fawzy et al., 1992). In the study area Abu Roash “G” Member consists of shale, limestone, sandstone, with siltstone streaks.

Tectonic setting

The structural patterns in north Western Desert from the Late Jurassic to Early Tertiary appear to have been influenced significantly by two primary tectonic forces related to Tethyan plate tectonics: (1) the sinistral shear during the Late Jurassic to Early Cretaceous and (2) the dextral shear during the Late Cretaceous to Paleocene time (Meshref et al., 1990) (Said, 1962).

The North-South trending seismic section (X Line 5625):

The seismic section is N-S direction of the study area (western side from study area) (Fig. 3) passing through Hm-18 St well projected and Hm-21well projected, which show interpreted seismic reflectors Apollonia Formation, Khoman Formation, Abu Roash

"A" Member, Abu Roash "C" Member, Abu Roash "F" Member and Middle Abu Roash "G" Member and Upper Bahariya Formation.

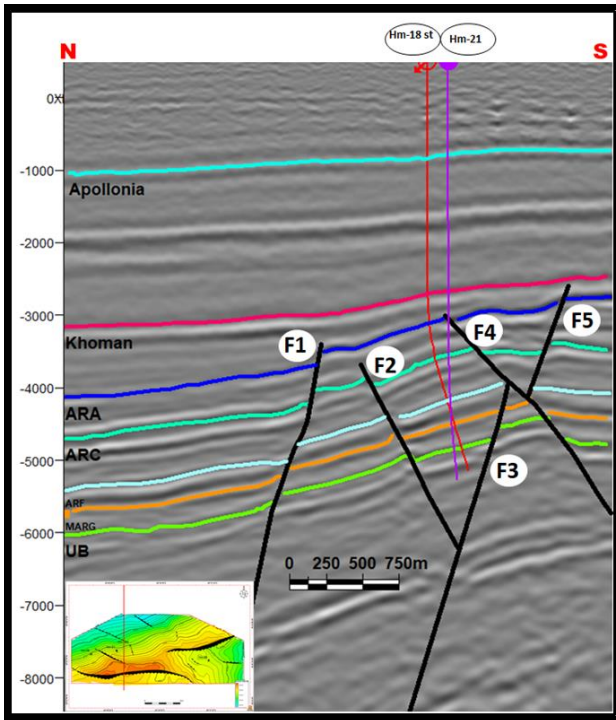


Fig. (3): N-S trending seismic section (5625) passing through Hm-18 St, Hm21 wells.

This section shows a NW-SE trending minor normal faults (F1, F2, F3, F5) and one Major normal fault E-W direction (F4), the major normal fault of Hamra field (F4) trending east-west direction which dip toward the south, cut members from above Abu Roash "A" to below Upper Bahariya Formation, which leading to form traps on the upthrown side, F1 cut members from above Abu Roash "A" to below Upper Bahariya Formation, F2 cut members from above Abu Roash "C" to below Upper Bahariya Formation, F3 cut members from Abu Roash "F" to below Upper Bahariya Formation, F5 mainor normal fault cut members from above Abu Roash "A" to below Abu Roash "F" members. Khoman is thicker in down thrown side which indicates a large accommodation space on the down thrown side of normal fault F1 is a syn-depositional fault at time of Khoman.

Structure contour maps

Structure contour maps constructed on the top Middle and Lower Abu Roash G sand Member (Figs. 4; 5) show that the contouring increment every 50 feet with values below -5250 feet. At the Northern side of map, and the highest values at the upthrown of the southern faults. Also the map shows the dipping toward Northwest.

This surface in the map could be structurally explained as Three-way dip closure bounded by the major normal faults E-W direction and some minor

ones, and three way dip closure in the eastern side, and other three-way dip closure in the eastern side bounded by the Major normal fault NE-SW direction.

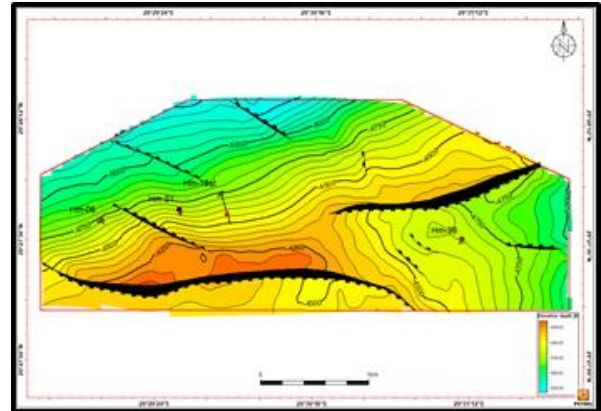


Fig. (4): Depth structure map on the top Middle Abu Roash G Member.

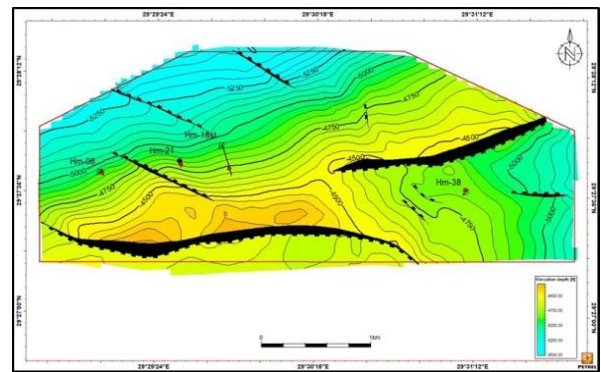


Fig. (5): Depth structure map on the top Lower Abu Roash G Member.

5-Well Log Analysis

Neutron Density crossplot

Abu Roash "G-10" zone represent the middle clastic reservoir zone of Abu Roash "G" Member, (Fig.6) shows the neutron density crossplots that have been applied on the Middle Abu Roash G zone. It is observed that, the reservoir sandstone plotted points are scattered and lay between sandstone and limestone lines with average grain density (Pma) 2.69 gm/cc and neutron porosity ranging from 25% to 33%. The zone is mainly reservoir sandstone with non-reservoir siltstone scattered and lays between limestone and dolomite lines. This indicates that the zone is mainly reservoir Calcareous sandstone with some non-reservoir siltstone scattered (Fig.7) shows the neutron density crossplots that have been applied on the Lower Abu Roash G sand zone. It is observed that, the major plotted points are scattered and lis between sandstone and limestone lines with average grain density (Pma) 2.69 gm/cc and neutron porosity ranging from 22% to 28%. The zone is mainly sandstone with non-reservoir siltstone. This indicates that the zone is mainly reservoir sandstone, clay and some limestone.

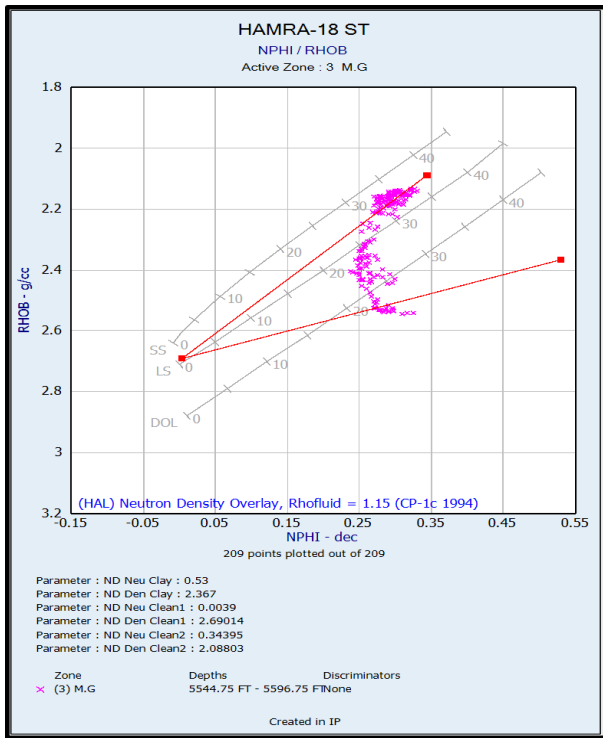


Fig. (6): Neutron density cross-plot showing the lithological components of the Middle Abu Roash "G" zone.

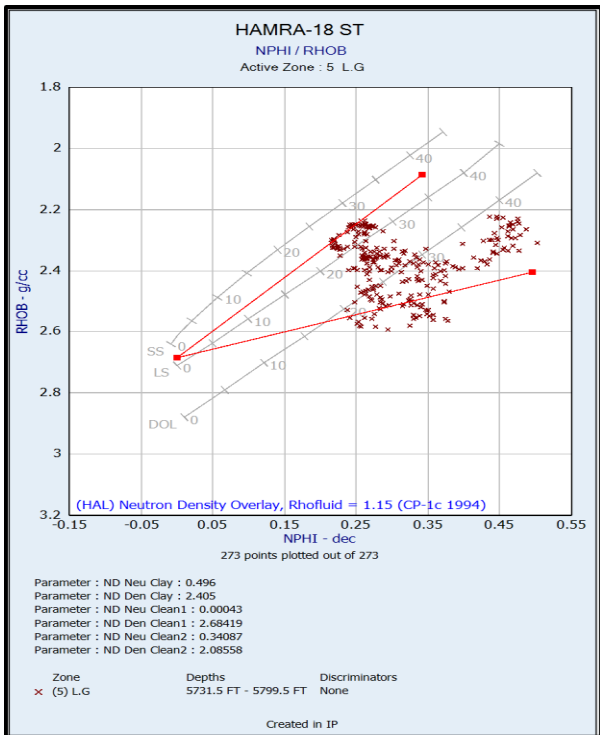


Fig. (7): Neutron density cross-plot showing the lithological components of the Lower Abu Roash "G" zone.

Well log analysis results

Zone	SW	Øeff	Vsh
ARG Reservoir	<=0.65	>=0.12	<=0.3

Table 1: Reservoir Cut-offs Applied in Hamra Field.

Zone Name	Net Pay	Thickness ft		AV Phi	Av Sw	AV Vcl
		Gross	Net			
Middle	12	51	27	26%	35%	12%
Lower	-	74	21	17%	91%	18%

Table 2: Reservoir Summary of Hamra-6 well.

Zone Name	Net Pay	Thickness ft		AV Phi	Av Sw	AV Vcl
		Gross	Net			
Middle	35	47	40	27%	37%	6%
Lower	10	69	21	19%	62%	15%

Table 3: Reservoir Summary of Hamra-18 St well.

Zone Name	Net Pay	Thickness ft		AV Phi	Av Sw	AV Vcl
		Gross	Net			
Middle	21	43	23	24%	34%	10%
Lower	-	72	27	20%	87%	13%

Table 4: Reservoir Summary of Hamra-21 well.

Zone Name	Net Pay	Thickness ft		AV Phi	Av Sw	AV Vcl
		Gross	Net			
Middle	15	39	19	24%	48%	8%
Lower	5	78	35	28%	52%	4%

Table 5: Reservoir Summary of Hamra-38 well.

6- Lateral variation of reservoir properties

After calculating the values of the log- parameters, the data have been averaged and mapped to represent their general distribution

Middle Abu Roash G ("G10" zone)

Abu Roash "G-10" zone represent the middle clastic reservoir zone of Abu Roash"G" Member, this zone is represented by reservoir sandstone and siltstone (Fig.12).

Abu Roash G-10 sandstones were deposited in prograding deltaic distributary environment and exhibit coarsening-upward profile with related increase in reservoir quality upwards. (Pasley et al., 2008).

The net reservoir sandstone isopach map of the Abu Roash "G-10" zone (Fig. 8) shows an increase towards the northern part of the study area especially with the maximum value (50 feet) and minimum value of (10 feet) in the eastern part, and southwest of the study area. This map shows two sandstone bodies separated by facies barrier (non-reservoir fine sandstone and siltstone) this barrier trending is Southwest direction.

From distribution pattern of net reservoir sandstone and the gradual upward decreasing in Gamma-ray log response which characterized this sandstone, bodies reflect an increase in depositional energy upward which characterizes the distributary river mouth bar facies (Emery and Myers.1996) (Cant. 1992) (coleman and prior. 1982), on other hand the area of low values of sandstone represent interdistributary fine sandstone and siltstone.

The effective porosity distribution map of the Abu Roash “G-10” (Fig. 9) shows an increase in the effective porosity toward the northern part of the study area and decrease toward the interdistributary fine sandstone and siltstone to the southwest, and eastern part of the study area. It reaches the maximum value (29%) at the mouth bar facies and the minimum (22%) toward the interdistributary fine sandstone and siltstone facies which reflects the effect of facies distribution on the effective porosity values.

Distribution of the clay volume (Fig.10) shows an increase of clay volume towards the southwest part of the study area fine sandstone and siltstone which reflects that clay volume is controlled by facies distribution.

The water saturation distribution map of the Abu Roash “G-10” zone (Fig.11) shows an increase towards the eastern, Southern part of the study area the water saturation decreases at the main closures of the study area reaching the minimum value (25%).

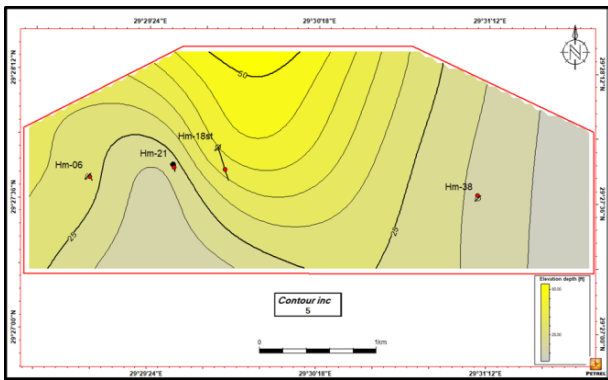


Fig. (8): Net reservoir Isopach map for Abu Roash”G-10” zone.

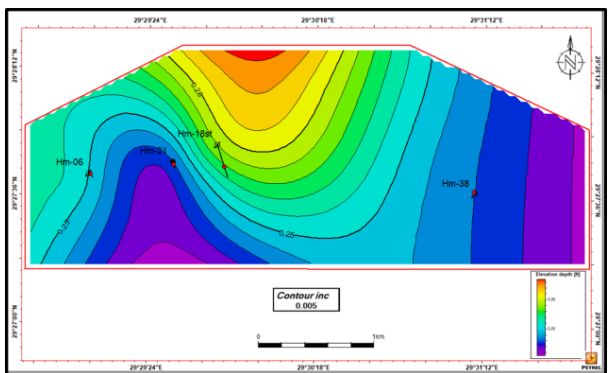


Fig. (9): Average effective porosity map for Abu Roash”G-10” zone.

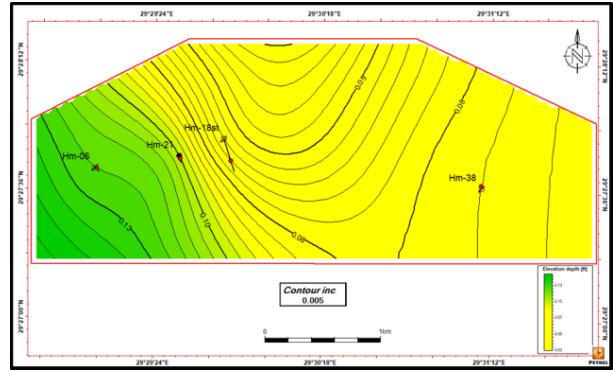


Fig. (10): Average clay volume distribution map for Abu Roash”G-10” zone

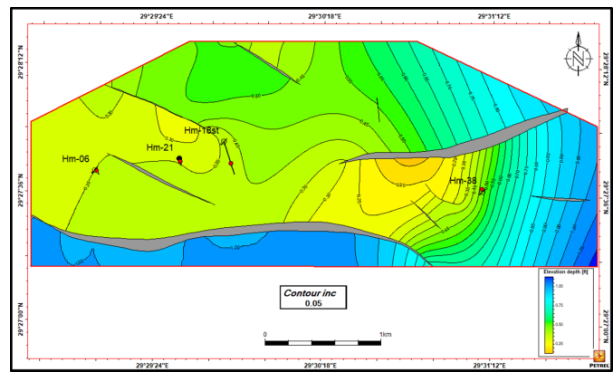


Fig. (11): Average water saturation map for Abu Roash”G-10” zone

Lower Abu Roash G (“G20”, “G21” “G22” zones)

Lower Abu Roash “G” was deposited entirely in shallow marine environment where the sands exhibit strong linear trends. These sands were apparently deposited in sub-tidal bars within a marine embayment.

This interval contains no evidence of incision at the base of the sands and the best sand facies exhibit current ripple cross-bedding, presumably from tidal currents (Pasley et al 2008).

Abu Roash “G-20” zone

The net reservoir sandstone isopach map of the Abu Roash “G-20 sand” (Fig. 13) shows an increase towards the eastern part of the study area especially, with the maximum value (16 feet) in the east direction, and minimum value (2 feet) to the western part of the study area. From the distribution pattern of net reservoir sandstone and the gradual upward increase in Gamma-ray log response which characterizes this sandstone. this body reflects a decrease in the depositional energy upward which characterizes the tidal creeks (Cant. 1992).

The effective porosity distribution map (Fig. 14) shows an increase in the effective porosity to the eastern part of the study area, reaching the maximum value (30%) which reflects the influences of facies distribution on effective porosity and decrease toward

the western part, and it reaches the minimum value (10 %) toward the west.

The clay volume distribution map (Fig. 15) shows an increase of clay volume towards the western part of the study area towards the low value of reservoir sandstone which indicates that clay volume distribution is controlled by facies distribution.

The water saturation distribution map (Fig.16) shows an increase towards the west part of the study area, where it reaches the maximum value (100%) The water saturation decreases towards the eastern part of the study area, reaching the minimum value (50%).The water saturation distribution is controlled by the structure element.

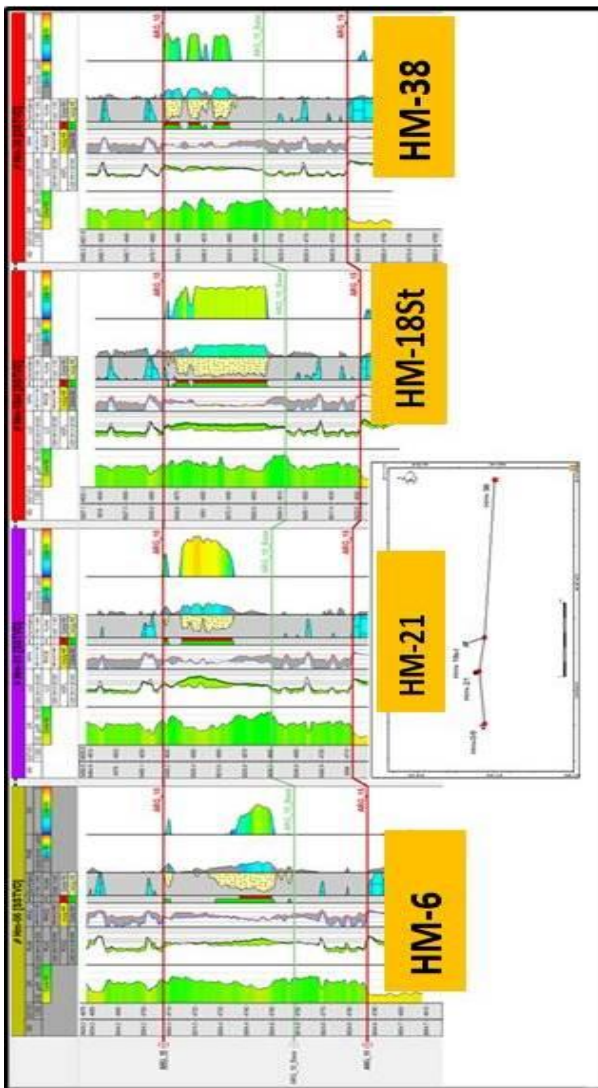


Fig. (12): Stratigraphic well-section flattened on top Abu Roash "G-10" shows the gradually upward decreasing of Gamma Ray response (sandstone coarsing upward).

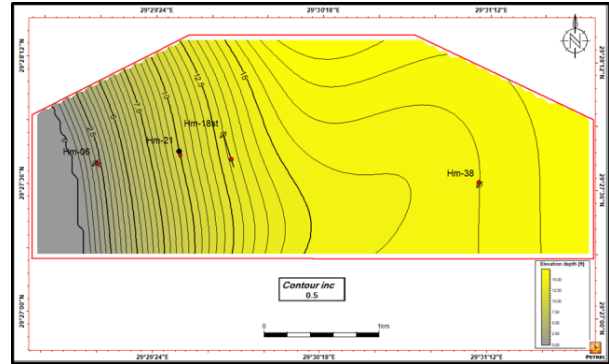


Fig. (13): Net reservoir Isopach map for Abu Roash" G-20" zone.

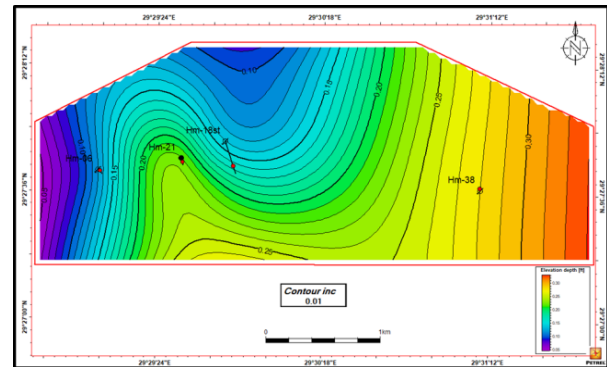


Fig. (14): Average effective porosity map for Abu Roash" G-20" zone.

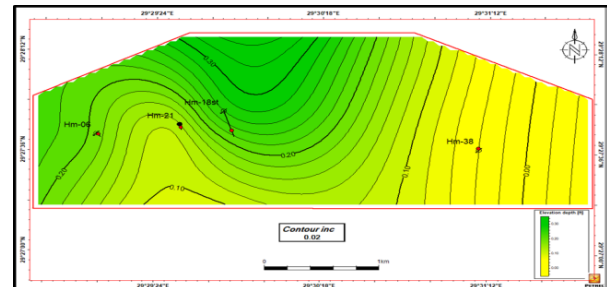


Fig. (15): Average clay volume distribution map for Abu Roash" G-20" zone.

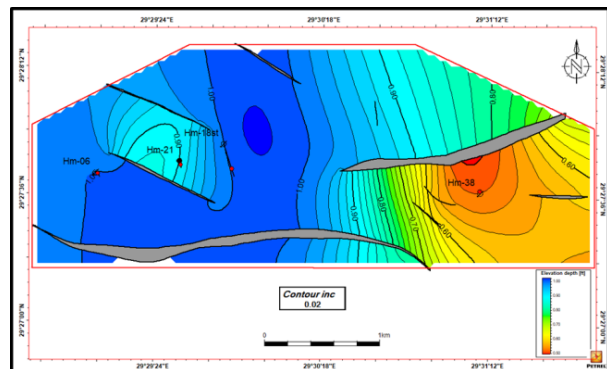


Fig. (16): Average water saturation map for Abu Roash" G-20" zone.

Abu Roash “G-21”zone

The net reservoir sandstone isopach map of the Abu Roash “G-21 sand” (Fig. 17) shows an increase towards the north and eastern part of the study area especially, with maximum value (10 feet) at north-east direction, and minimum value (6 feet) to the southwest part of the study area.

The effective porosity distribution map (Fig. 18) shows an increase in the effective porosity to the northern part of the study area, reaches the maximum value (22%) which reflects the influences of facies distribution on effective porosity and decreases towards the eastern part and the southwest, where it reaches the minimum value (19 %)

The clay volume distribution map (Fig. 19) shows a decrease of clay volume towards the northern part of the study area where it reaches the minimum value (10 %) which indicates that the clay volume distribution controlled by facies distribution.

The water saturation distribution map (Fig.20) shows an increase towards the western part and eastern part of the study area, where it reaches the maximum value (100%).The water saturation decreases toward the central part of the study area reaching the minimum value (50%). Water saturation distribution is controlled by a structural element.

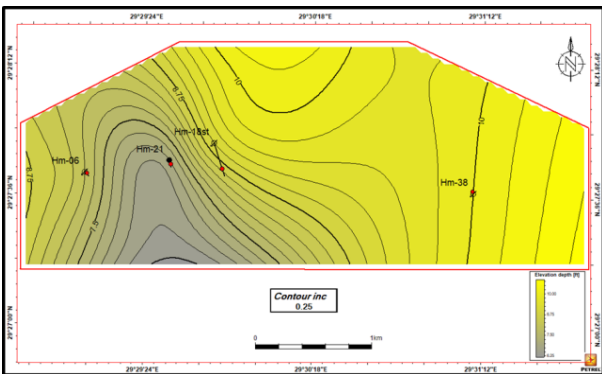


Fig. (17): Net reservoir Isopach map for Abu Roash”G-21” zone.

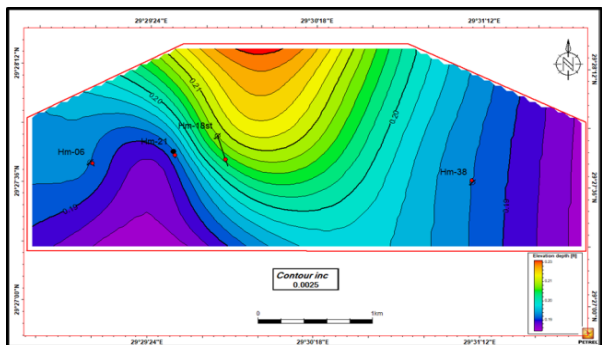


Fig. (18): Average effective porosity map for Abu Roash”G-21” zone.

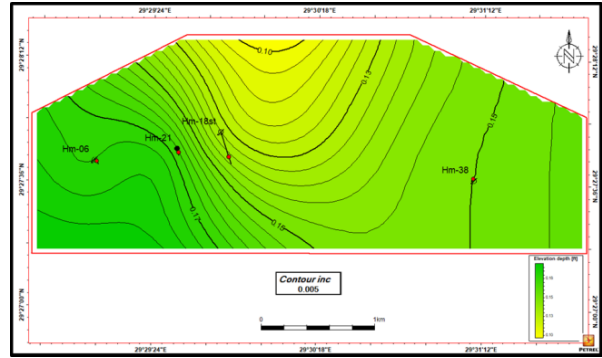


Fig. (19): Average clay volume distribution map for Abu Roash” G-21” zone.

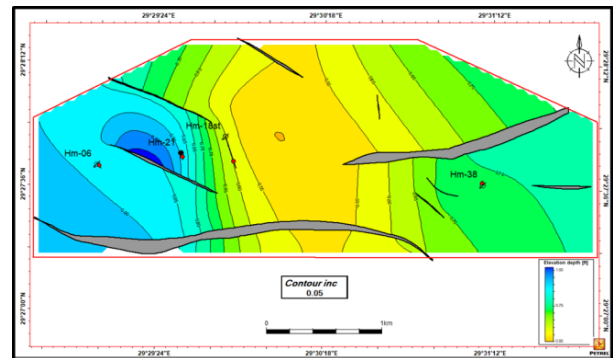


Fig. (20): Average water saturation map for Abu Roash”G-21” zone.

Abu Roash “G-22”zone

The net reservoir sandstone isopach map of the Abu Roash “G-22 sand” (Fig. 21) shows an increase towards the central part of the study area especially, with maximum value (15 feet) in the northern direction, and minimum value (7 feet) to the eastern part of the area.

The effective porosity distribution map (Fig.22) shows an increase in the effective porosity to the central part of the area, reaching the maximum value (25%) to the north direction which reflects the influences of facies distribution on effective porosity and decreases towards the eastern part, it reaches the minimum value (17 %).

The clay volume distribution map (Fig. 23) shows a decrease of clay volume towards the central part of the area towards the high value of reservoir sandstone which indicates that clay volume distribution is controlled by facies distribution.

The water saturation distribution map (Figure 24) shows an increase towards the western part of the area, where it reaches the maximum value (100%) The water saturation decreases toward the central part of the area reaching the minimum value (50%).Water saturation distribution is controlled by a structural element.

Lower Abu Roash “G” represents the lower clastic reservoir zone of Abu Roash” Member, This zone

represented by reservoir sandstone and siltstone. Lower Abu Roash “G-” is classified into “G- 20” sand, and “G- 21” sand and “G- 22” sand zones based on the reservoir sandstone quality (Fig. 25).

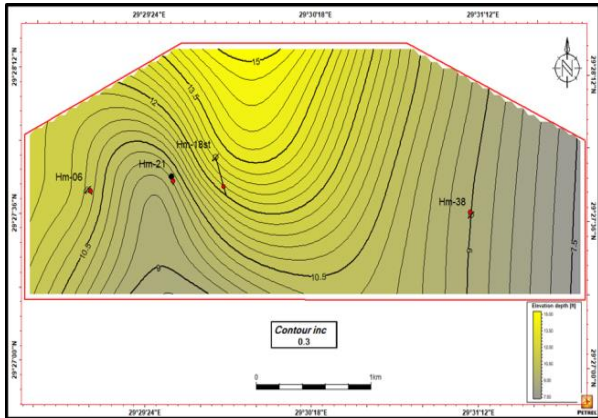


Fig. (21): Net reservoir Isopach map for Abu Roash “G-22” zone.

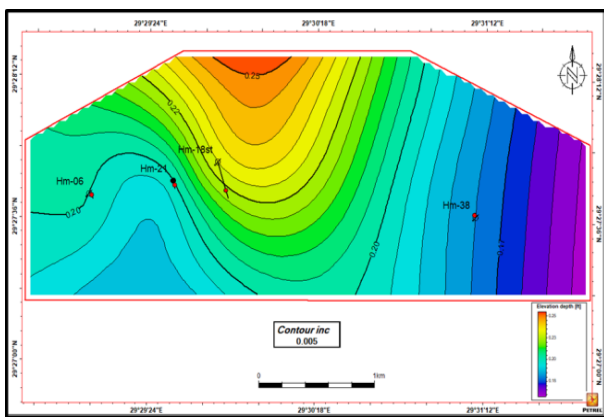


Fig. (22): Average effective porosity map for Abu Roash “G-22” zone.

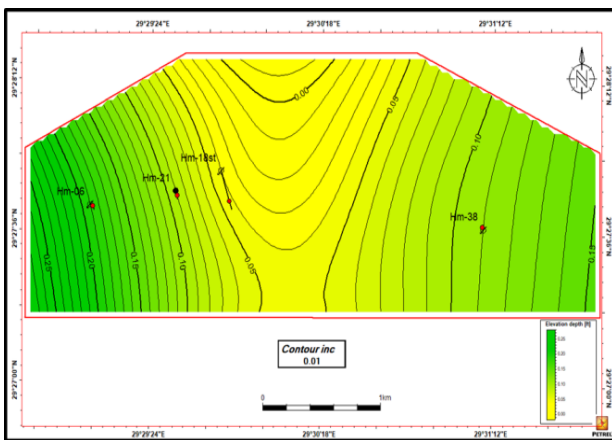


Fig. (23): Average clay volume distribution map for Abu Roash “G-22” zone.

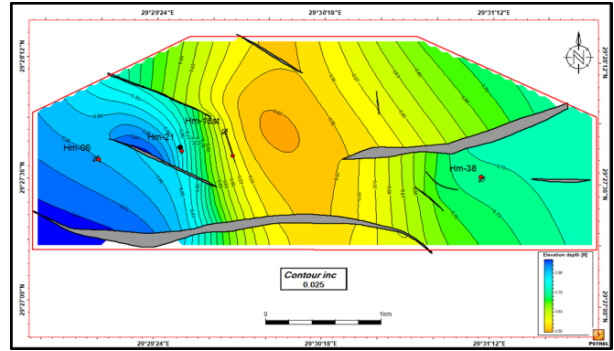


Fig. (24): Average water saturation map for Abu Roash “G-22” zone

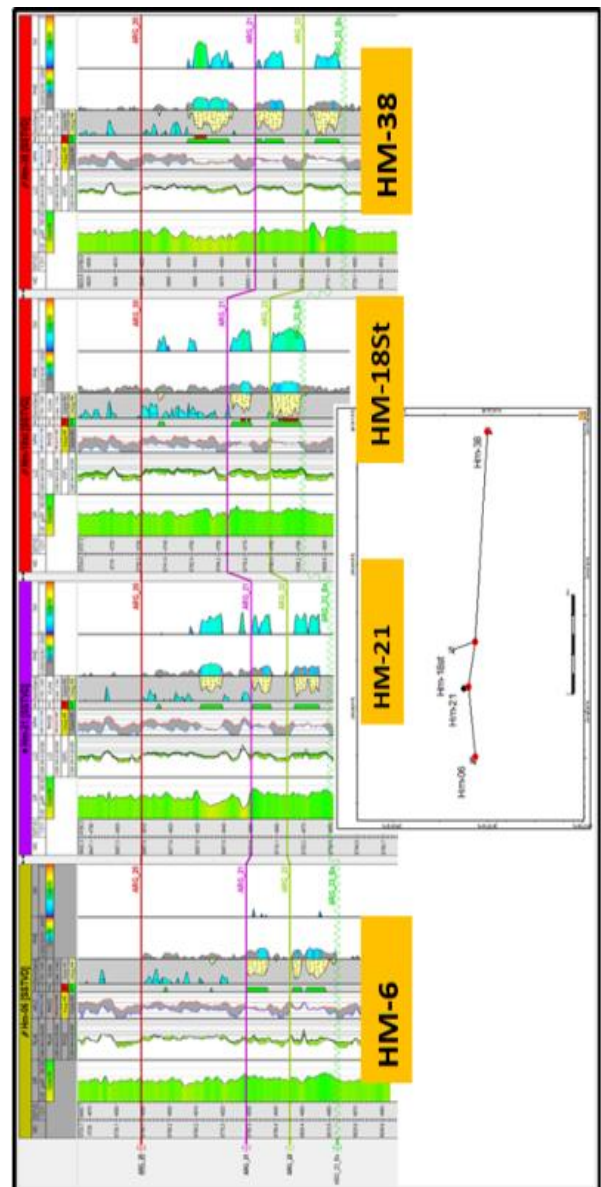


Fig. (25): Stratigraphic well-section flattened on top Lower Abu Roash G shows the fining upward of Gamma Ray log response

7-Hydrocarbons Volume calculation

Preliminary hydrocarbon volumes have been estimated for Middle Abu Roash 'G' Member ("G-10") and Lower Abu Roash 'G' Member ("G-20", "G-21", "G-22"). The reservoir input parameters were based on the sums and averages from the first four drilled wells penetrating the reservoir section. These estimations were calculated based upon the following formula expressed in terms of stock tank of original oil in place (STOOIP): $STOOIP (STB) = 7758 * A * h * \Phi_{eff} * (1 - S_w) * N/G * 1/B_o$ Where, A= reservoir area in acres, h= net pay thickness in feet, Φ_{eff} =effective porosity in fraction, $(1 - S_w)$ = hydrocarbon saturation in fraction, N/G = net to gross reservoir ratio, B_o = formation volume factor and 7758 is an acre foot conversion for oil. The cumulative stock tank of original oil in place STOOIP estimated for zones is 28.208 Million Stock Tank Barrel separated as follow:

Zone	STOOIP MMSTB
G-10	18
G-20	5.701
G-21	2.575
G-22	1.932
Cumulative	28.208

Table 5: The stock tank of original oil in place STOOIP estimated for zones.

8. Conclusions

The principal structure responsible for hydrocarbon entrapment in the study area was a structural high which corresponds to the three-way dip closure of east-west major normal fault and the northeast-southwest normal fault of Hamra oil field area. The petrophysical study was conducted to identify the productive zone, to distinguish between oil, and water in the reservoir, and to define the petrophysical parameters to be used later on petrophysical model. The analysis showed pay zones in (Middle Abu Roash (G) Member, and Lower Abu Roash (G) Membe.

All zones after calculating clay volume, water saturation, and average effective porosity and after applying cut-offs, encountered net pays as follows, 12 feet cumulative net pay for Hamra-6, 45 feet cumulative net pay for Hamra-18 St, 21 feet cumulative net pay for Hamra-21, and 20 feet cumulative net pay for Hamra-38.

Mapping the petrophysical characteristics of the different reservoirs encountered in the study area shows that the water saturation controlled by the structural elements at Lower Abu Roash 'G' Member ("G-20", "G-21", "G-22" zones), and Middle Abu Roash 'G' Member ("G-10") is controlled by a combination of structure and facies elements. Clay volume and effective

porosity of all zones is controlled by facies distribution. Zones are controlled by facies distribution.

Based on the cumulative stock tank of original oil in place STOOIP estimated for zones is 28.208 Million Stock Tank Barrel of oil.

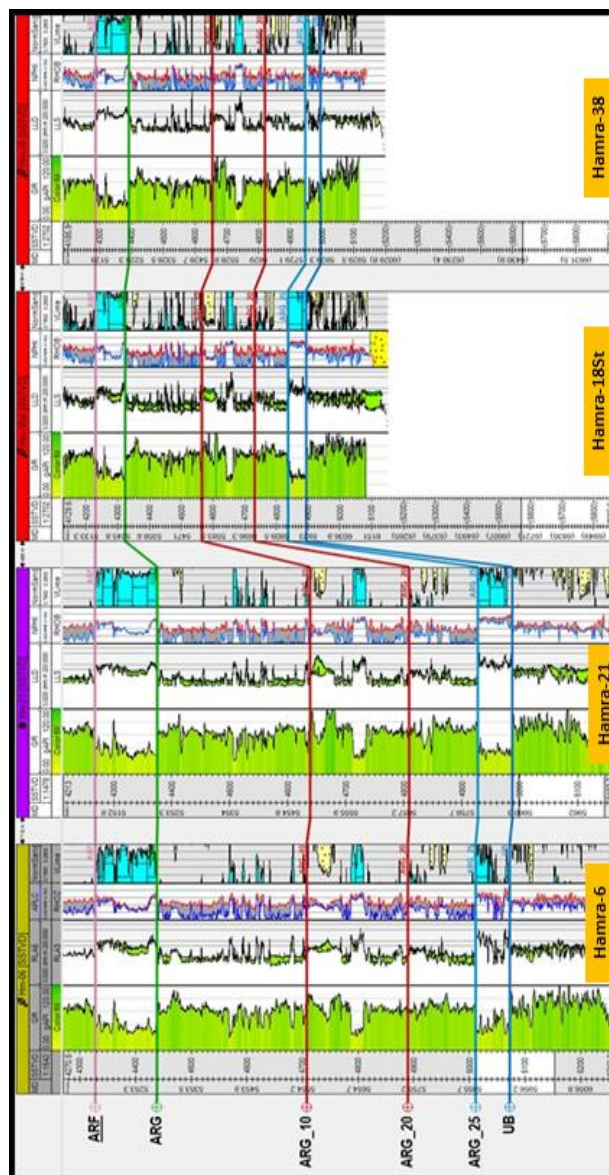


Fig. (26): Stratigraphic correlation chart among Hamra wells.

9-Acknowledgement

A word of gratitude is extended to the Egyptian Petroleum Corporation (EGPC), Qarun Petroleum Company (QPC). Sincere thanks to all the staff of Menofiya University.

REFERENCES

- Abdel Aal, A., (1990):** Subsurface study of the Abu Gharadig basin, Western Desert, Egypt, Msc. Thesis, Ain Shams University.
- Cant, D.J., (1992):** subsurface facies analysis, in Walker, R.G., and James, N.P. eds., facies

models:response to sea level change :Geological association of Canada, st. John;s, new-foundland, P 27-45

Coleman, J.M., & Prior, D.B. (1982). Deltaic environment in sandstoned epositional nvrionments; Amer. Assoc. petroleum geol.,Mem. 31.

Emery, D., Myers, K.J. (1996): Sequence Stratigraphy. Blackwell, Oxford, England.

Fawzy, A., and Dahi, M. (1992): Regional geological evaluation of the Western Desert, Egypt: Paper presented at the Geology of the Arab World, Cairo University, pp.111-149.

Hantar, G., North Western Desert, In Said, R. (1990): Geology of Egypt, (A.A. Balkema, Rotterdam, Brookfiled, pp.293-320.

Moustafa, A.R., Saudi, A., Moubasher, A., Ibrahim, I.M., Molokhia, H., and Schwartz, B. (2003): "Structural setting and tectonic evolution of the Bahariya Depression, Western Desert, Egypt".No.16, 244p.

Moustafa, A.R. (2008): Mesozoic-Cenozoic Basin Evolution in the Northern Western Desert of Egypt. Geology of East Libya, vol. 3, , pp. 35-42.

Pasley, M.A., Gabe A. and Nassef, O. and Joe C. (2008): Depositional Facies Control on Reservoir Characteristics in the Middle and Lower

Abu Roash "G" Sandstones, Western Desert, Egypt. Adapted from oral presentation at AAPG International Conference and Exhibition, Cape Town, South Africa, October 26-29, 2008.

Said, R., (1962): Tectonic framework of Egypt. In Said, R. (eds.). The geology of Egypt. Elsvier publishing company.

Schlumberger, (1995): Geology of Egypt Paper presented at the Well Evaluation Conference, Schlumberger, Cairo, pp. 58-66. [2].

Meshref, W.M, (1990): Tectonic framework of Egypt. In Said, R. (Ed.), Geology of Egypt, 113-156, Balkema, Rotterdam.